Supplementary Material: Polarimetric Neural Field via Unified Complex-Valued Wave Representation

Chu Zhou[1] Yixin Yang[2,3] Junda Liao[1,4] Heng Guo[5] Boxin Shi[2,3*] Imari Sato[1,4*]

[1]National Institute of Informatics, Japan

[2]State Key Laboratory of Multimedia Information Processing, School of Computer Science, Peking University, China

[3]National Engineering Research Center of Visual Technology, School of Computer Science, Peking University, China

[4]Graduate School of Information Science and Technology, University of Tokyo, Japan

[5]School of Artificial Intelligence, Beijing University of Posts and Telecommunications, China

zhou_chu@hotmail.com, {yangyixin93, shiboxin}@pku.edu.cn,

liao-junda@g.ecc.u-tokyo.ac.jp, guoheng@bupt.edu.cn, imarik@nii.ac.jp

A. Discussions About the Conventions

In this section, we provide discussions about the conventions for polarimetric parameters, corresponding to Footnote 2 of the main paper.

Malus' law [1] describes the relationship between the polarized image $\mathbf{I}_\alpha$ (captured using a linear polarizer at angle α) and the polarimetric parameters (including the total intensity (TI) $\mathbf{I}$, degree of polarization (DoP) $\mathbf{p}$, and angle of polarization (AoP) $\boldsymbol{\theta}$). Depending on the convention [9], it can be expressed as:

$$\mathbf{I}_\alpha = \frac{\mathbf{I}}{2} \cdot (1 - \mathbf{p} \cdot \cos(2(\alpha - \boldsymbol{\theta}))), \tag{A}$$

which is adopted in our work and in previous studies [7, 8] (denoted as **Convention1**), or as

$$\mathbf{I}_\alpha = \frac{\mathbf{I}}{2} \cdot (1 + \mathbf{p} \cdot \cos(2(\boldsymbol{\theta} - \alpha))), \tag{B}$$

which is used by pCON [5] (denoted as **Convention2**). Besides, the Stokes parameters [2] also have two different definitions. Denoting $\mathbf{I}_{\alpha_{1,2,3,4}}$ as the polarized images captured at $\alpha_{1,2,3,4} = 0°, 45°, 90°, 135°$, the Stokes parameters $\mathbf{S}_{0,1,2}$ are defined as

$$\begin{cases} \mathbf{S}_0 = \mathbf{I}_{\alpha_1} + \mathbf{I}_{\alpha_3} = \mathbf{I}_{\alpha_2} + \mathbf{I}_{\alpha_4} \\ \mathbf{S}_1 = \mathbf{I}_{\alpha_3} - \mathbf{I}_{\alpha_1}, \text{ and } \mathbf{S}_2 = \mathbf{I}_{\alpha_4} - \mathbf{I}_{\alpha_2} \end{cases} \tag{C}$$

if we follow Convention1, and defined as

$$\begin{cases} \mathbf{S}_0 = \mathbf{I}_{\alpha_1} + \mathbf{I}_{\alpha_3} = \mathbf{I}_{\alpha_2} + \mathbf{I}_{\alpha_4} \\ \mathbf{S}_1 = \mathbf{I}_{\alpha_1} - \mathbf{I}_{\alpha_3}, \text{ and } \mathbf{S}_2 = \mathbf{I}_{\alpha_2} - \mathbf{I}_{\alpha_4} \end{cases} \tag{D}$$

if we follow Convention2. Since in polarimetric imaging, polarimetric parameters are typically estimated as

$$\mathbf{I} = \mathbf{S}_0, \mathbf{p} = \frac{\sqrt{\mathbf{S}_1^2 + \mathbf{S}_2^2}}{\mathbf{S}_0} \text{ and } \boldsymbol{\theta} = \frac{1}{2}\arctan(\frac{\mathbf{S}_2}{\mathbf{S}_1}), \tag{E}$$

the estimated TI $\mathbf{I}$ and DoP $\mathbf{p}$ remain the same under both Convention1 and Convention2. However, the estimated AoP $\boldsymbol{\theta}$ would be different due to the sensitivity of $\arctan$ to small numerical errors (*i.e.*, despite the arguments being mathematically equivalent ($\frac{\mathbf{I}_{\alpha_4} - \mathbf{I}_{\alpha_2}}{\mathbf{I}_{\alpha_3} - \mathbf{I}_{\alpha_1}} = \frac{\mathbf{I}_{\alpha_2} - \mathbf{I}_{\alpha_4}}{\mathbf{I}_{\alpha_1} - \mathbf{I}_{\alpha_3}}$), the limited precision of floating-point arithmetic and the bounded range of $\arctan$ can lead to small discrepancies, especially when dealing with values close to the boundaries).

Here, we also provide some qualitative comparisons with pCON [5], which follows Convention2 (the convention used by pCON [5]). Note that both our method and pCON [5] are retrained using polarimetric parameters according to Convention2. Besides, we also visualize the DoP and AoP directly, using the same visualization approach employed by pCON [5], instead of using color maps as in our main paper. Results are shown in Fig. A, where we can see that our method produces fewer artifacts and noise patterns compared with pCON [5].

B. Additional Qualitative Comparisons

In this section, we provide additional qualitative comparisons with pCON [5], FINER [4], and S-INR [3], corresponding to Footnote 3 of the main paper. The results are shown in Fig. B and Fig. C.

Besides, since the polarized images provided by pCON [5] are captured by polarization cameras, to evaluate the generalization ability of our method, we also provide qualitative comparisons using the polarized images captured via

*Corresponding authors.

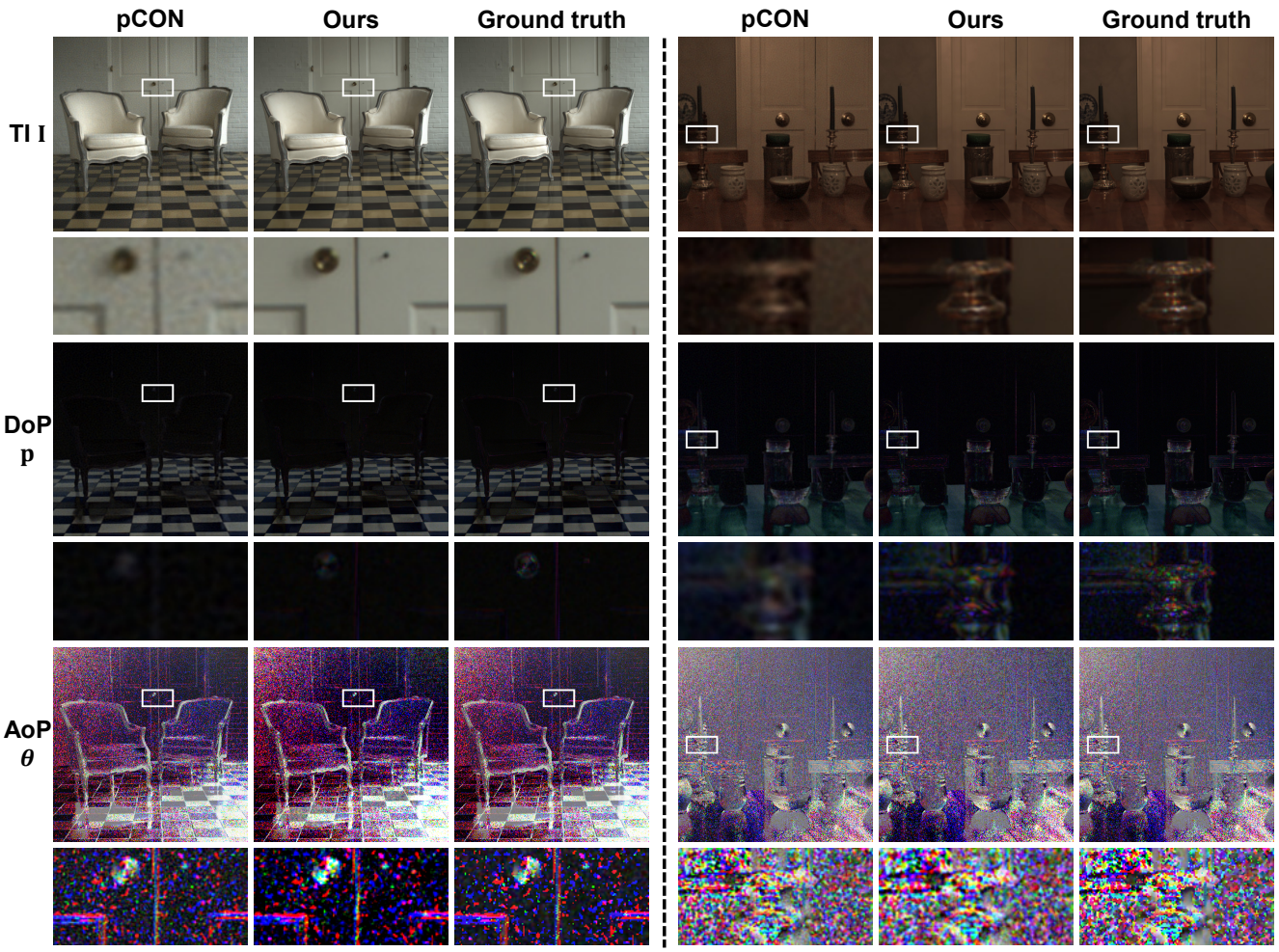

Figure A. Qualitative comparisons with pCON [5] following the convention used by pCON [5] (Convention2). The DoP and AoP are visualized directly, following the same visualization approach employed by pCON [5], instead of using color maps as in our main paper. Please zoom in for better details.

rotating a polarizer [6]. The results are shown in Fig. D and Fig. E.

C. Additional Results of Polarized Image Rendering

In this section, we provide additional qualitative comparisons on the accuracy of the rendered polarized images with pCON [5], FINER [4], and S-INR [3], corresponding to Footnote 4 of the main paper. The results are shown in Fig. F (the rendered polarized images at $\alpha_1 = 0°$) and Fig. G (the rendered polarized images at $\alpha_2 = 45°$).

Besides, we provide the quantitative evaluations for all selected polarizer angles ($\alpha_{1,2,3,4} = 0°, 45°, 90°, 135°$) in Tab. A. From the results, we can see that our method outperforms all compared methods for all polarizer angles.

D. Additional Results of Super-Resolution Querying

In this section, we provide additional qualitative comparisons of the super-resolution querying performance with pCON [5] and FINER [4], corresponding to Footnote 5 of the main paper. Specifically, we fit the polarimetric parameters at a resolution of 1024×1024 and query them at 2048×2048. Note that here we cannot compare with S-INR [3], since it supports querying only at the resolution used for fitting. The results are shown in Fig. H.

References

[1] Eugene Hecht. *Optics*. Pearson Education India, 2012. 1

[2] GP Können. *Polarized light in nature*. CUP Archive, 1985. 1

[3] Jiayi Li, Xile Zhao, Jianli Wang, Chao Wang, and Min Wang. Superpixel-informed implicit neural representation for multi-

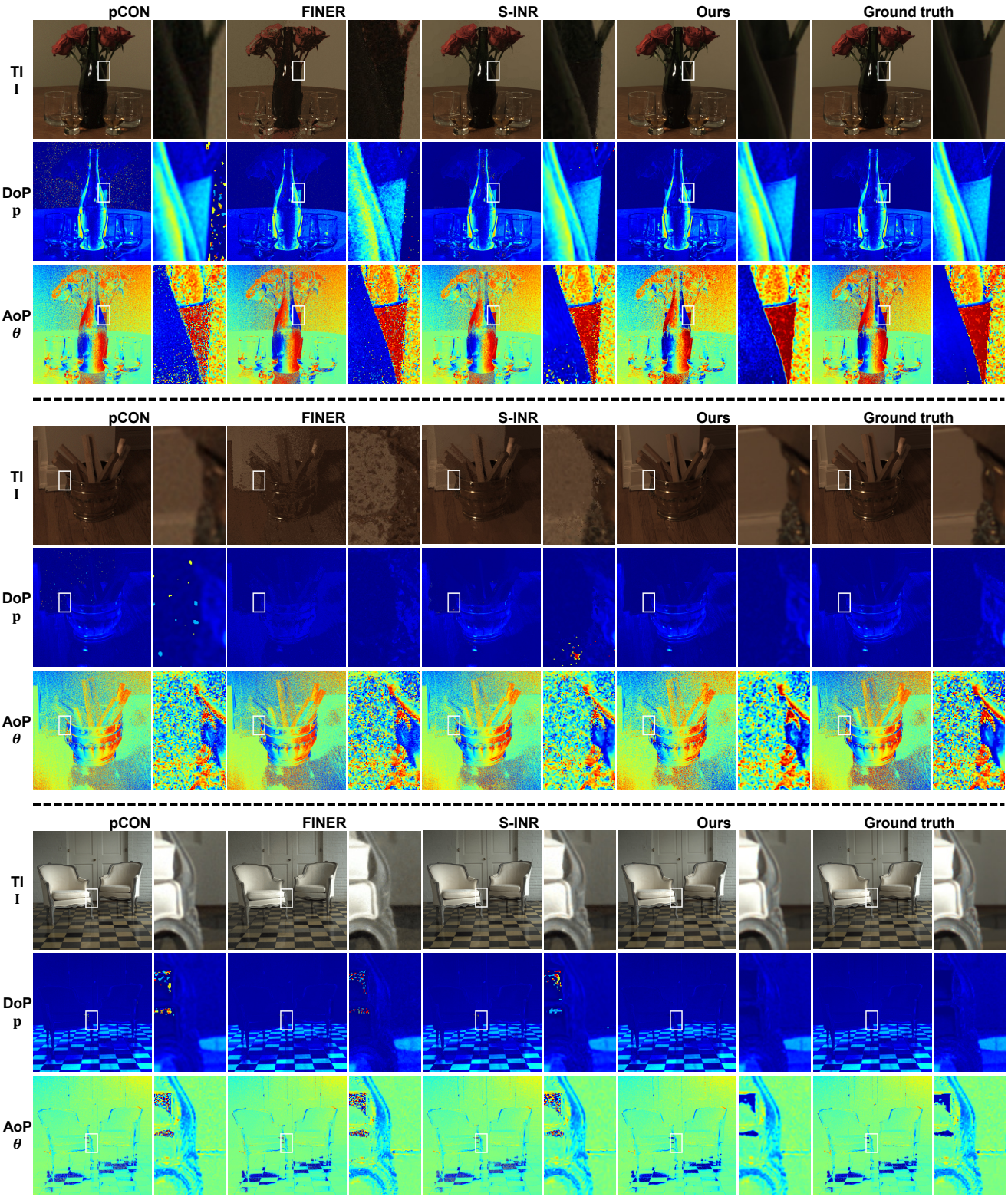

Figure B. Additional qualitative comparisons with pCON [5], FINER [4], and S-INR [3] (part 1). Please zoom in for better details.

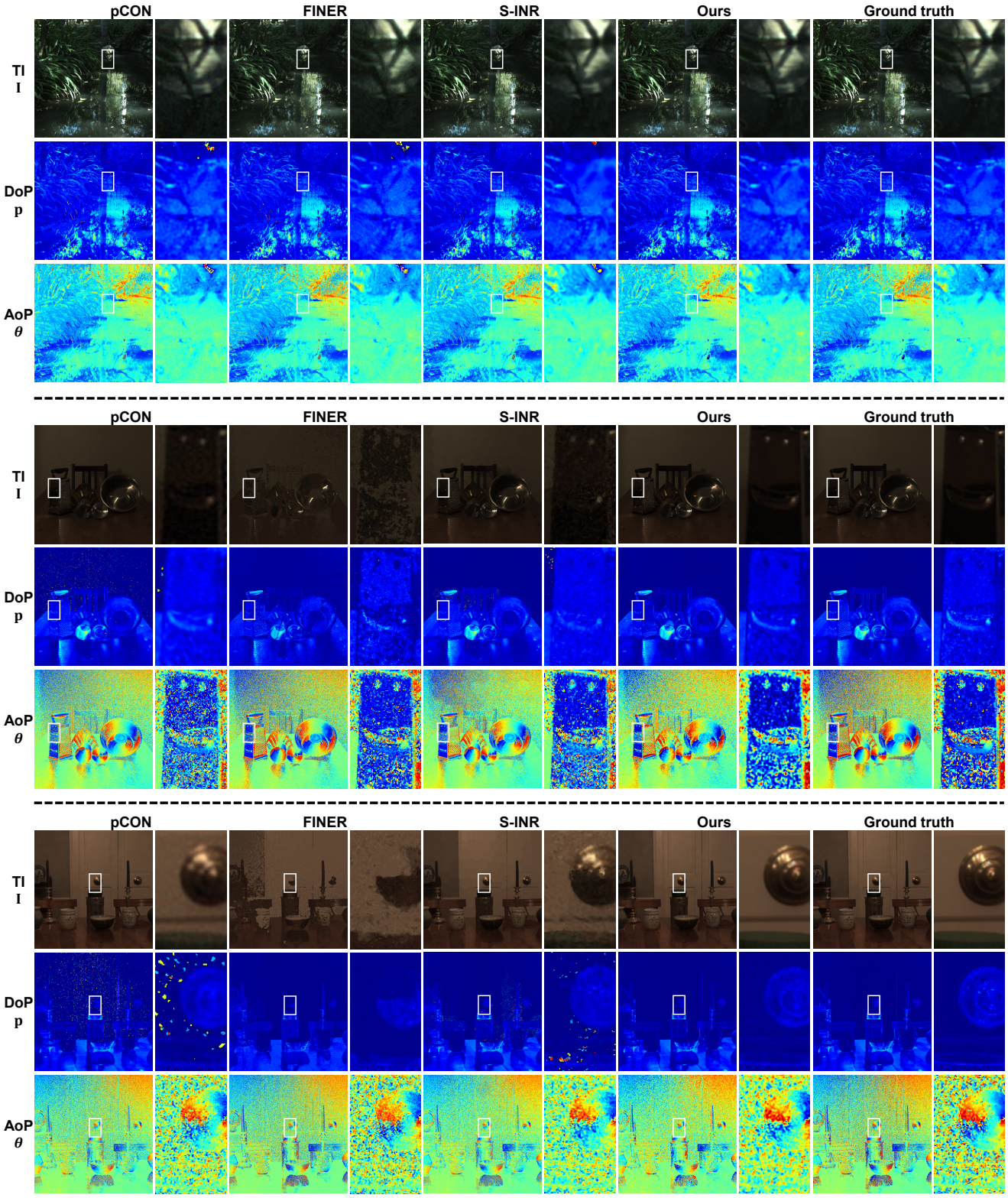

Figure C. Additional qualitative comparisons with pCON [5], FINER [4], and S-INR [3] (part 2). Please zoom in for better details.

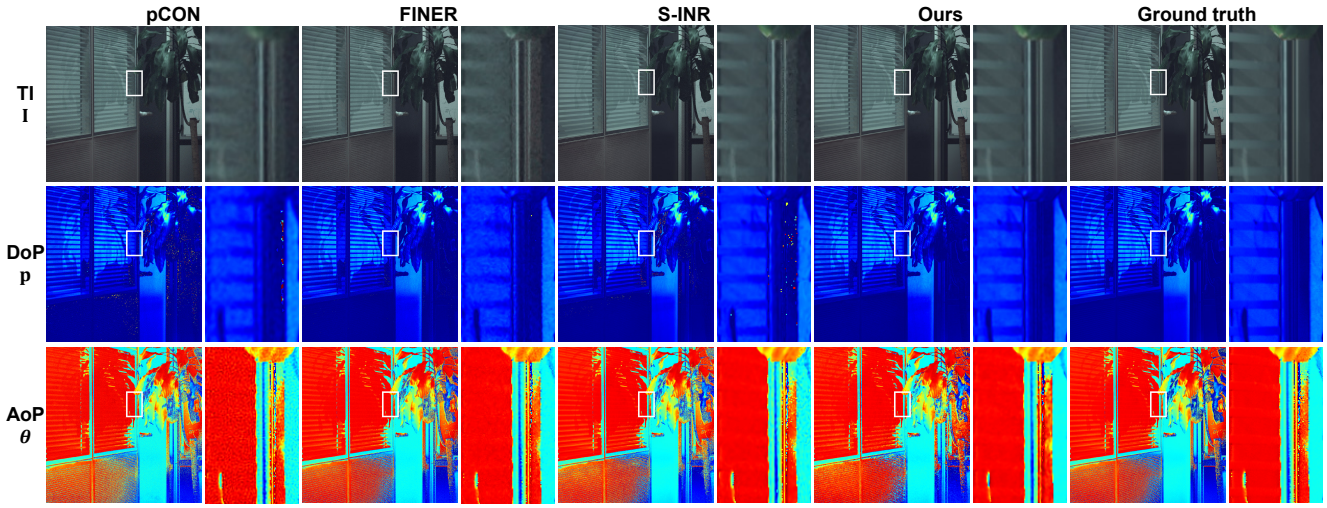

Figure D. Qualitative comparisons with pCON [5], FINER [4], and S-INR [3] using the polarized images captured via rotating a polarizer [6] (part 1). Please zoom in for better details.

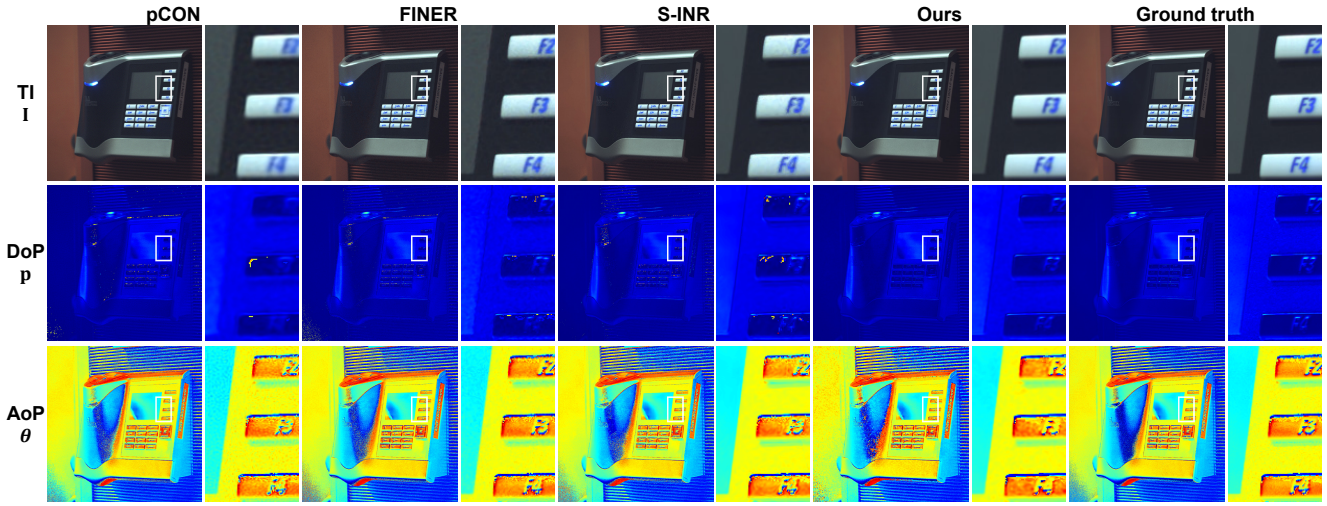

Figure E. Qualitative comparisons with pCON [5], FINER [4], and S-INR [3] using the polarized images captured via rotating a polarizer [6] (part 2). Please zoom in for better details.

dimensional data. In *Proc. of European Conference on Computer Vision*, pages 258–276, 2024. 1, 2, 3, 4, 5, 6

[4] Zhen Liu, Hao Zhu, Qi Zhang, Jingde Fu, Weibing Deng, Zhan Ma, Yanwen Guo, and Xun Cao. FINER: Flexible spectral-bias tuning in implicit neural representation by variable-periodic activation functions. In *Proc. of Computer Vision and Pattern Recognition*, pages 2713–2722, 2024. 1, 2, 3, 4, 5, 6, 7

[5] Henry Peters, Yunhao Ba, and Achuta Kadambi. pCON: Polarimetric coordinate networks for neural scene representations. In *Proc. of Computer Vision and Pattern Recognition*, pages 16579–16589, 2023. 1, 2, 3, 4, 5, 6, 7

[6] Simeng Qiu, Qiang Fu, Congli Wang, and Wolfgang Heidrich. Linear polarization demosaicking for monochrome and colour polarization focal plane arrays. In *Computer Graphics Forum*, pages 77–89, 2021. 2, 5

[7] Yoav Y Schechner, Srinivasa G Narasimhan, and Shree K Nayar. Instant dehazing of images using polarization. In *Proc. of Computer Vision and Pattern Recognition*, pages I–I, 2001. 1

[8] Chu Zhou, Minggui Teng, Youwei Lyu, Si Li, Chao Xu, and Boxin Shi. Polarization-aware low-light image enhancement. In *Proc. of the AAAI Conference on Artificial Intelligence*, pages 3742–3750, 2023. 1

[9] Evgenij Zubko and Ekaterina Chornaya. On the ambiguous definition of the degree of linear polarization. *Research Notes of the AAS*, 3(3):45, 2019. 1

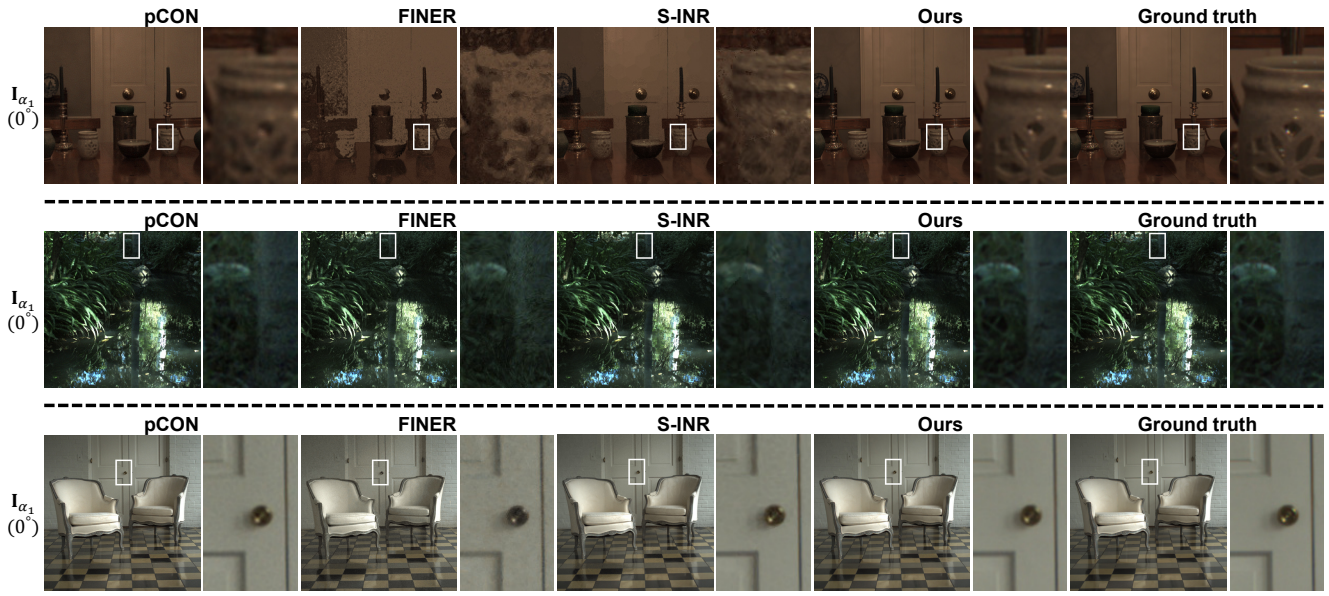

Figure F. Additional qualitative comparisons on the accuracy of the rendered polarized images with pCON [5], FINER [4], and S-INR [3] (part 1). Here, we show the rendered $\mathbf{I}_{\alpha_1}$ (the polarized images at $\alpha_1 = 0°$). Please zoom in for better details.

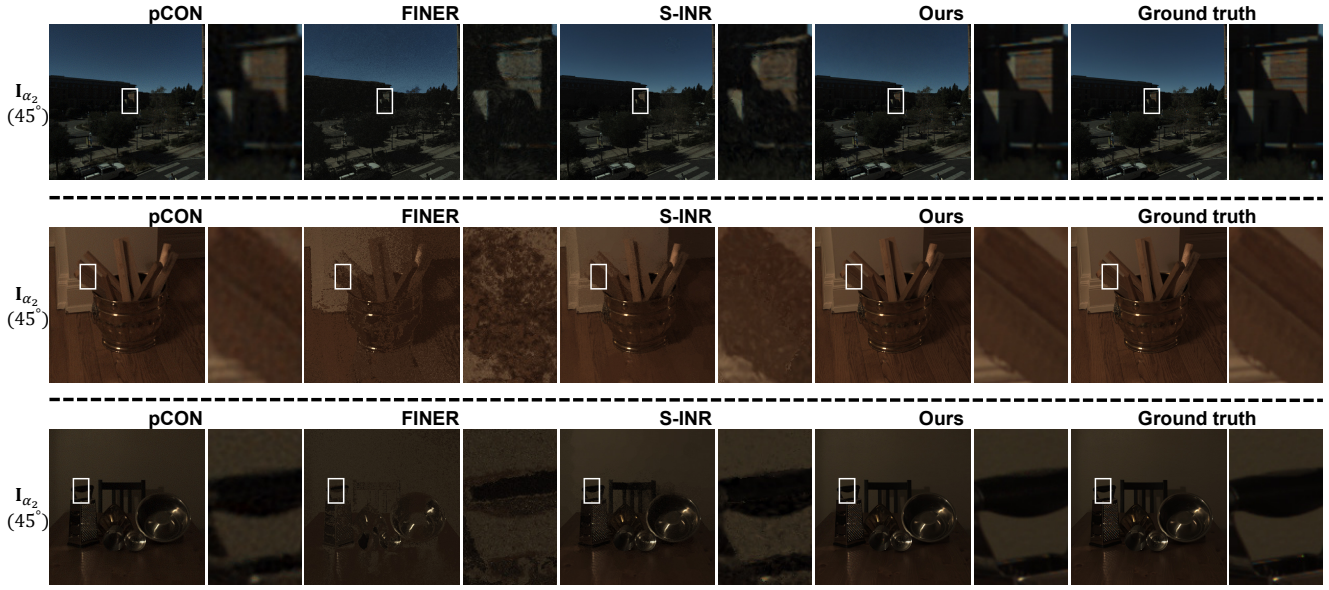

Figure G. Additional qualitative comparisons on the accuracy of the rendered polarized images with pCON [5], FINER [4], and S-INR [3] (part 2). Here, we show the rendered $\mathbf{I}_{\alpha_2}$ (the polarized images at $\alpha_1 = 45°$). Please zoom in for better details.

Table A. Quantitative comparisons on the accuracy of the rendered polarized images with pCON [5], FINER [4], and S-INR [3].

	PSNR↑/SSIM↑ of $\mathbf{I}_{\alpha_1}$ (0°)				PSNR↑/SSIM↑ of $\mathbf{I}_{\alpha_2}$ (45°)				PSNR↑/SSIM↑ of $\mathbf{I}_{\alpha_3}$ (90°)				PSNR↑/SSIM↑ of $\mathbf{I}_{\alpha_4}$ (135°)			
	pCON [5]	FINER [4]	S-INR [3]	Ours	pCON [5]	FINER [4]	S-INR [3]	Ours	pCON [5]	FINER [4]	S-INR [3]	Ours	pCON [5]	FINER [4]	S-INR [3]	Ours
Building	**36.58**/0.884	33.24/0.820	36.45/**0.909**	**39.11**/**0.931**	**36.72**/**0.910**	31.99/0.784	35.65/0.900	**42.78**/**0.971**	**36.27**/0.881	32.81/0.810	36.16/**0.907**	**39.04**/**0.932**	**38.61**/**0.932**	34.23/0.856	37.24/0.921	**43.67**/**0.974**
Firewood	**39.46**/**0.949**	27.22/0.641	36.59/0.914	**47.60**/**0.989**	**39.55**/**0.949**	27.36/0.645	36.58/0.914	**47.74**/**0.989**	**39.52**/**0.949**	27.41/0.647	36.49/0.912	**47.50**/**0.989**	**39.55**/**0.949**	27.32/0.645	36.59/0.914	**47.75**/**0.989**
Grater	**37.92**/**0.946**	27.72/0.729	36.85/0.933	**44.72**/**0.987**	**37.91**/**0.946**	27.76/0.726	36.89/0.934	**45.01**/**0.986**	**38.01**/**0.948**	27.77/0.725	36.81/0.933	**44.88**/**0.987**	**38.19**/**0.946**	27.78/0.728	37.04/0.934	**45.20**/**0.986**
Pottery	**38.04**/**0.947**	27.82/0.734	35.62/0.915	**44.41**/**0.985**	**38.33**/**0.946**	28.08/0.742	35.87/0.918	**44.42**/**0.981**	**38.55**/**0.949**	28.25/0.753	35.87/0.917	**44.90**/**0.985**	**38.34**/**0.945**	28.04/0.742	35.85/0.917	**44.44**/**0.981**
Stream	**35.85**/**0.936**	32.80/0.867	34.88/0.922	**39.88**/**0.981**	**37.18**/**0.939**	34.21/0.879	36.37/0.931	**40.81**/**0.981**	**37.61**/**0.938**	34.71/0.879	36.66/0.933	**42.26**/**0.983**	**35.88**/**0.932**	32.93/0.864	35.03/0.924	**39.51**/**0.980**
Sunroom	**41.22**/**0.966**	35.14/0.891	39.76/0.959	**44.16**/**0.986**	**41.91**/**0.970**	35.71/0.903	40.21/0.963	**44.44**/**0.987**	**41.68**/**0.969**	35.85/0.908	40.06/0.962	**44.32**/**0.987**	**41.79**/**0.970**	35.59/0.902	40.07/0.963	**44.33**/**0.987**
Valentines	34.98/**0.919**	28.44/0.767	**35.26**/0.918	**41.70**/**0.979**	35.14/0.914	28.48/0.757	**35.32**/**0.918**	**40.82**/**0.969**	**35.36**/**0.924**	28.47/0.759	35.23/0.917	**41.85**/**0.980**	35.11/0.914	28.46/0.761	**35.34**/**0.918**	**40.82**/**0.969**

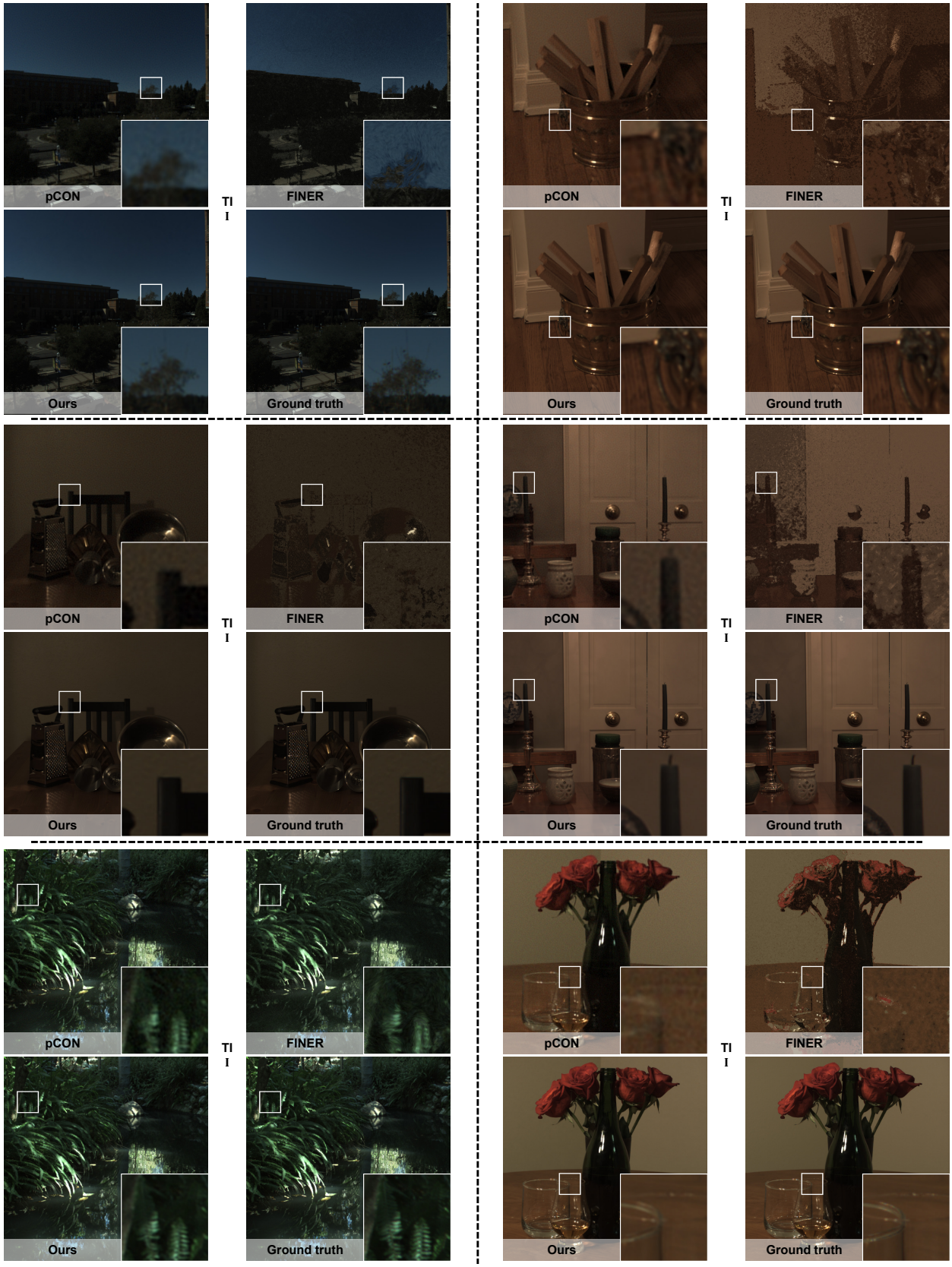

Figure H. Additional qualitative comparisons of the 2× super-resolution querying performance with pCON [5] and FINER [4].